

Passive seismic survey on the Darquain oil field

Mohammad Reza Saadatmand¹, Ali Moradi^{1, *}, Hosein Hashemi¹

1- Institute of Geophysics, University of Tehran, Iran.

* Corresponding Author: asmoradi@ut.ac.ir

Received: 15 September 2013 / Accepted: 11 November 2013 / Published online: 15 November 2013

Abstract

In the form of passive seismic methods, broadband seismometers have been used in hydrocarbon exploration. The frequency bandwidth typically studied is in the range of 1–6 Hz. The observations on low frequency band of microtremors are used to calculate the spectral ratio of vertical and horizontal components (V/H) and Power Spectral Density (PSD). Attributes based on the V/H ratio and the PSD have been suggested as tools to identify hydrocarbon reservoir location. In this paper, earthquakes and background noise recorded by broadband seismometers are used. We used ambient noise data and a major earthquake data (Nurabad, Iran) that were recorded in a seismographic network with five broadband seismometer stations located at Darquain Oil Field in Khuzestan, Iran. At a station located on top of the reservoir we observe a prominent peak in both V/H and PSD attributes.

Keywords: Passive Method, Borehole Geophysics, Darquain, PSD, V/H Method.

1–Introduction

In recent years, new geophysical tools have been recruited for exploration of hydrocarbon resources. One of these methods is the application of passive seismic data as a complementary tool to conventional active seismic methods. In passive methods, random spread spectrum noise and some distinguished recorded earthquakes in broadband seismic networks are employed to study reservoirs (Rode *et al.*, 2010).

The results of passive seismic projects alone, especially those could be associated with shallow layer effect, still in doubt (Green and Greenhalgh, 2009; Lambert *et al.*, 2009). It's obvious that the proposed method cannot be expected to respond fully as an alternative to 3D seismic methods but it can be regarded as a complementary tool to distinguish the potentials of hydrocarbon reservoirs. In passive seismic methods, there is no artificial source but natural phenomena are used instead. An example of

such phenomena is using local earthquakes phase data used in passive seismic tomography (Zhang *et al.*, 2009) or in the calculation of PSD (Power Spectral Density) attributes (Nguyen *et al.*, 2008). Another example of these data is the ambient seismic signal received by broadband receivers (Saenger *et al.*, 2009). Dangel *et al.* (2003) found that there are significant energy anomalies in low frequency bandwidth (between 1.5 – 4 Hz) of passive seismic data over a hydrocarbon reservoir. Furthermore, Saenger *et al.* (2008), Nguyen *et al.* (2008), Saenger *et al.* (2009), Lambert *et al.* (2009) and Graf *et al.* (2007) also investigated energy anomaly in the frequency range of about 1–6 Hz. In order to describe this anomaly in detail, they proposed several attributes such as PSD–IZ (Power Spectral Density–Integrated Vertical component), V/H, polarization, and maximum peak frequency. These attributes exhibit anomalous values above the known hydrocarbon accumulations that shown these

attributes can improve probabilities identifying hydrocarbon reservoirs. In some studies, these attributes were successfully used in early stages of exploration. Lambert *et al* (2007) correlated amplifications in the V/H-ratio along three profiles with a real reservoir boundary (Lambert *et al* (2011)).

Other energy sources are earthquakes which produce all kinds of seismic waves in a wide frequency band that can interact with a hydrocarbon reservoir. Some earthquakes are used for calculating PSD in three time sections: before, during, and after an earthquake (Nguyen *et al.*, 2008). The aim is to test for a prominent peak over the oil field after the earthquake which is different from the time before the earthquake arrival. Accordingly, it can be said that passive seismic methods may be regarded as a complementary tool in full waveform imaging of seismic field.

Data from a five-station network of broadband stations, which one of them are located near the production wells of Darquain oil field was a chance to examine this methods in this area. In the current study, the vertical to horizontal (NS and EW components) spectral ratio at five site locations, each equipped with 3C seismometers, is calculated over the Darquain oil field of Iran. We also use the polarization technique to analyze the directivity of the background noise (Riahi *et al*, 2013).

2-Overview of general geology and reservoir horizons in Darquain oil field

The Dezful Embayment and Abadan Plain (SW Iran) contain major parts of the remaining Iranian oil reserves (Motiei, 1995). These oil provinces are characterized by two types of structural closure: very gentle N-S to NE-SW trending basement-cored anticlines (Arabian-type highs) in the SE, and open to tight, NW-SE-trending thrust-related folds in the NE (Zagros Fold-Thrust Belt; ZFTB) (Abdollahie Fard *et al.*, 2006.)

The Darquain structure is part of the Mesopotamian-Persian Gulf lowland (Berberian, 1995) and structurally belongs to the stable shelf of the Arabian platform. Its trend is in contradiction to the Zagros type structures (NW-SE). The Darquain structure with N-S trend is located 45km NE of Abadan in Southwestern Iran (Fig. 1). This zone is not seismically active and there are no significant geological outcrops for subsurface structures; therefore, our data are based on geophysical activities (AbdollahieFard *et al.*, 2006).

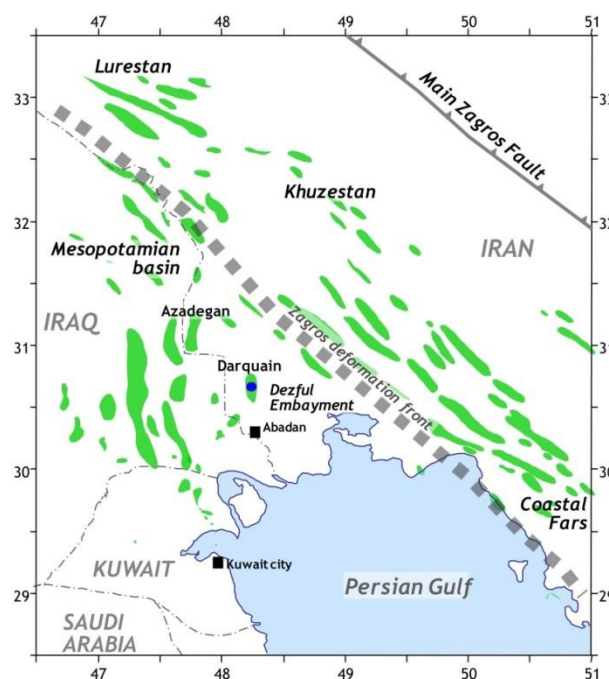


Figure 1) All known oil fields in southwestern Iran (green areas). The Darquain oil field is indicated by a blue spot and is located north of Abadan.

The Darquain dome is a broad and gentle anticline with four-way structural closure in the Jurassic and Cretaceous strata (Maleki *et al.*, 2006). The N-S trending structures of Abadan plain such as Darquain are basement-involved horst systems. Drill-hole and seismic data from the Darquain anticline demonstrate unconformities and erosional surfaces due to uplifting of basement-cored horsts. The main reservoirs in Darquain oil field are Bangestan and Khami including Ilam, Sarvak, and Fahlian formations (Motiei, 1995). The Ilam Formation (Santonian-Campanian) is composed of limestone containing mudstone, wackestone,

and partly argillaceous limestone to shaly intercalations. Sarvak Formation (Senomanian) is mainly composed of limestone with some shaly intercalations. The Fahlian Formation (Neocomian) is mainly composed of pure and argillaceous limestone with some shaly intercalations.

3– Data and method

The data used in this study were recorded during August 2010 and August 2011 at the Darquain seismographic network which consists of five stations. The stations are equipped with GURALP SYSTEMS instruments. The Sensors and digitizers are broadband CMG–3ESPC three–component seismometers and 24–bit CMG–DM24 digitizers, respectively.

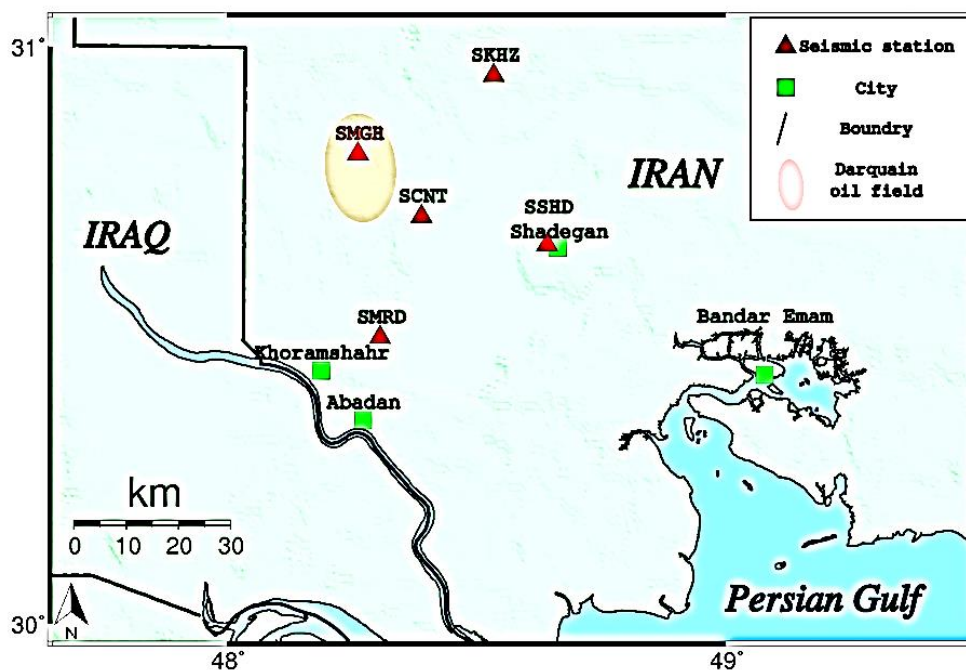


Figure 2) Location of five stations (red triangles) and Darquain oil field.

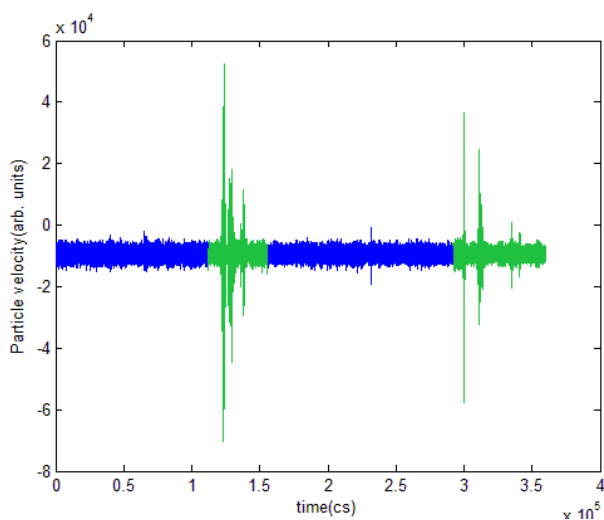


Figure 3) Time series of vertical particle velocity of seismic motion (sampling period is 10 ms) for SMGH station. Background data (blue) was used for further calculation while signal periods with events (green) were removed. (cs is hundredths of second).

At each site, signals were recorded with a sampling rate of 100 Hz, and data were recorded on a separate file every hour. The digitizer time synchronize to GPS time with external GPS receivers and the recording system had a flat frequency response between 0.03 and 50 Hz.

Figure 2 shows the position of the five stations with respect to the Darquain oil field, with the SMGH station located on top of the reservoir. Furthermore, while the SCNT station is on the eastern boundary of the reservoir the three other stations (SMRD, SSHD, and SKHZ) are out of the oil field boundaries. The three outer stations are contaminated with some cultural noise.

4– Data analysis

4.1–V/H spectral ratio

Calculation of V/H is derived from the H/V ratio used to characterize microtremors (Bard, 1999; Konno and Ohmachi, 1998; Nakamura, 1989) which in the current study we applied as a

tool for oil industry. Separating background noise from other phenomena (cultural noise and earthquake) is an important first step in the workflow.

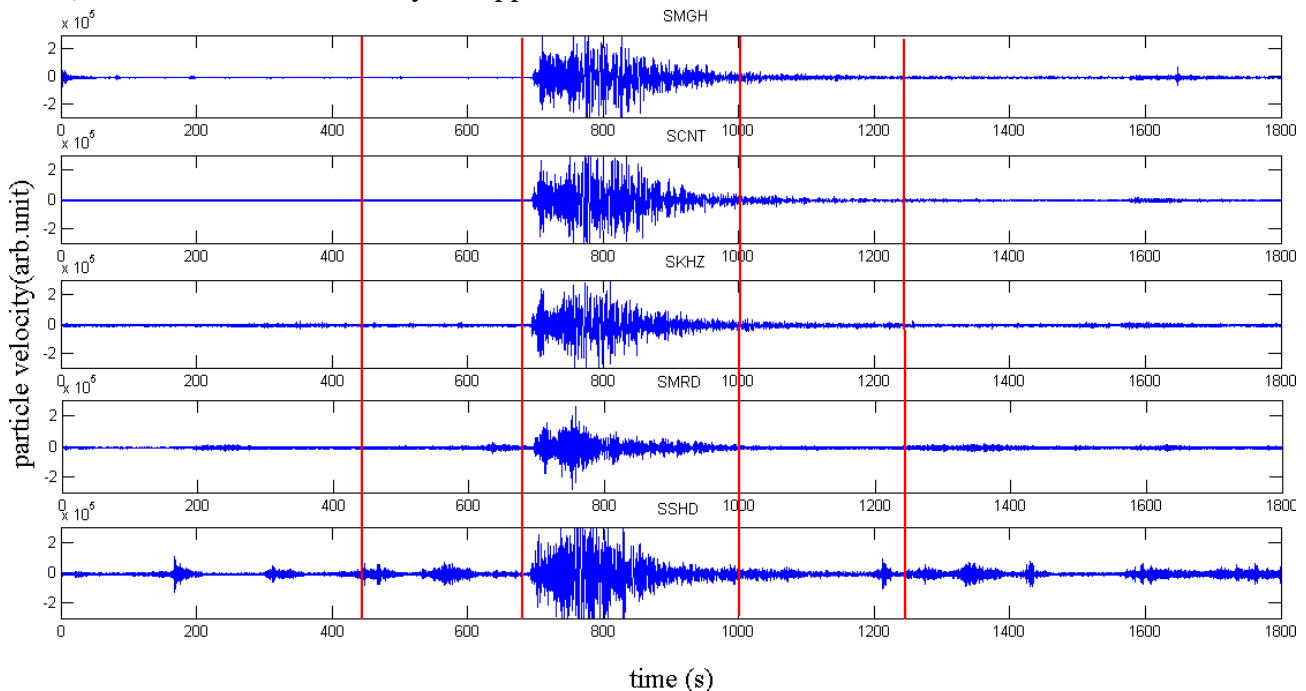


Figure 4) The seismogram observations of the Nurabad earthquake on the vertical component of the five stations of the Darquain network. Red lines indicate different time sections.

For example as it seen in Figure 3 we remove the artificial noise if the amplitude of signals exceed three time more than average amplitude for having more flat data we use the waveforms witch recorded between 9 PM to 3 AM local time. After removing Earthquake and artificial noise we divided data to 10 minutes windows each windows analysis separately. The processing flow for every window is low pass filtering, calculation of spectral amplitudes, smoothing, and then calculating V/H for every window. For each station we combined all windows and averaged the V/H values. The result of calculated spectral ratio for all five stations is presented in black line in V/H diagram in Figures from 5-a to 9-a.

4.2-PSD_IZ (Power Spectral Density_Vertical component)

Another attribute that we investigated in this survey is PSD of Z components which are calculated for January 05, 2011 Nurabad earthquake (MW= 5.4) that occurred in at Fars province, Iran. The distance from this earthquake epicenter to the center of the

Darquain seismographic network is about 350 km. The earthquake waveforms in Z component of all stations are shown in Figure 4.

A PSD for vertical seismograms was calculated in three time sections (before, during, and after the earthquake) according to the red lines in Figure 4. This earthquake was happened at 9:25:27 in local time, first window duration is 270 seconds that began at 9:20:30, next window that involve the earthquake, chosen a window with length 390 seconds, is from 9:25:00 to 9:31:30 and last window duration is 270 seconds that began from 9:31:30 to 9:36:00. The results can be observed in Figures from 5-b to 9-b. As we can see in Figure 4, the length and magnitude of coda wave are different in stations due to local structure beneath of stations. The PSD processing flow consist low pass filtering (butterworth filtering with 4 poles and corner frequency of 10 Hz) and computing the PSD-IZ attribute of each window. The results illustrate that the SMGH station demonstrates a peak at 3 Hz after the earthquake but not before it; this is a notable finding.

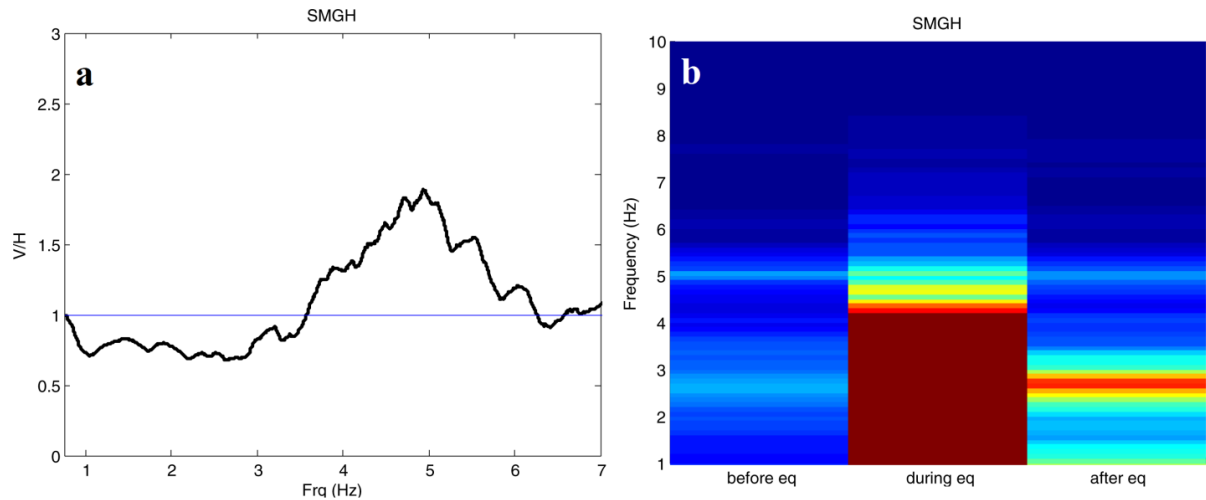


Figure 5) Analysis frequency of SMGH station located upon known reservoir. (a) There is a peak between 4–6 Hz in the V/H ratio, (b) there is a significant peak around 3 Hz after the earthquake in PSD diagram (red spectrum is the largest power, blue is the lowest).

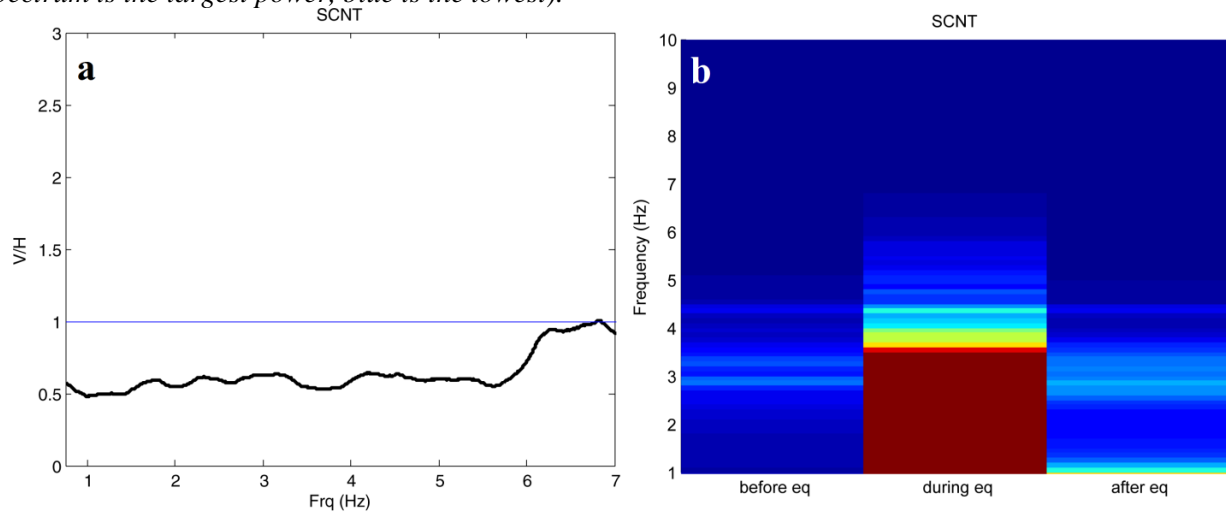


Figure 6) Analysis frequency of SCNT station located alongside known reservoir. a) There is no peak in considering frequency (1–6 Hz) in the V/H ratio diagram. b) There is very little increasing between 2.5–4 Hz after the earthquake in PSD diagram.

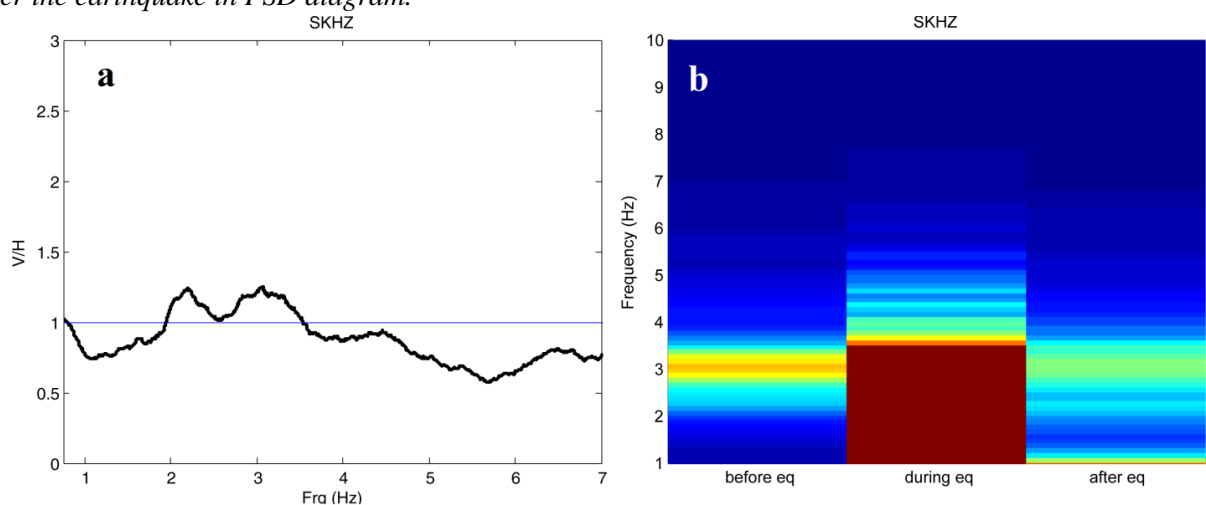


Figure 7) Analysis frequency of SKHZ station located in the unknown area. (a) there is a peak in 2–3.5 Hz in the V/H ratio diagram (b) there is a significant peak around 3 Hz before and after the earthquake in PSD diagram, but in after section, it is less.

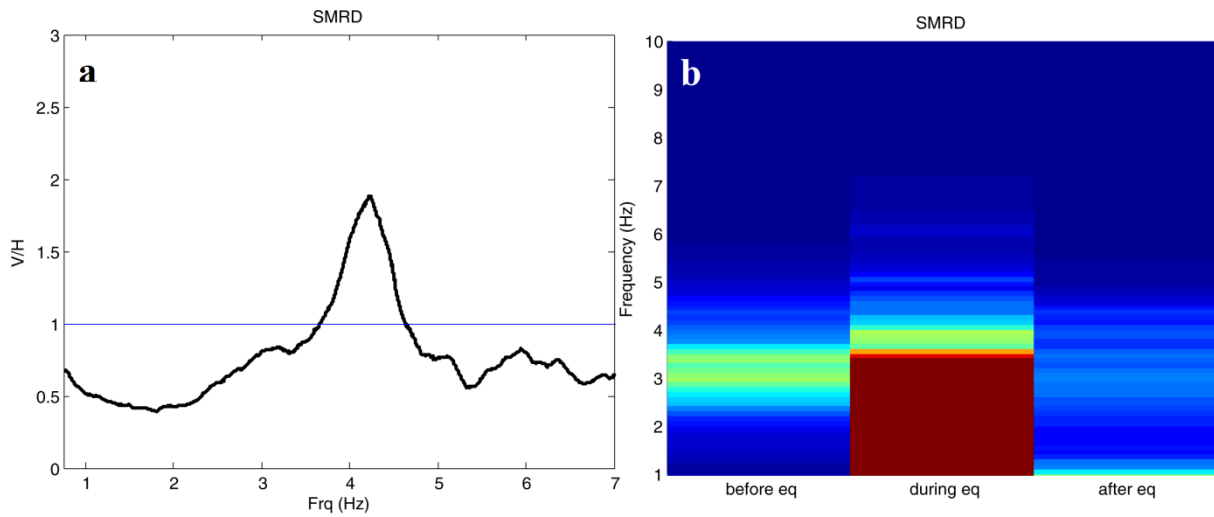


Figure 8) Analysis frequency of SMRD station located in the unknown area. (a) there is a narrow peak in 4.2 Hz in the V/H ratio diagram (b) there is not any significant peak after the earthquake in frequency range between 1.5–4 Hz in PSD diagram, but there is a little in the before section

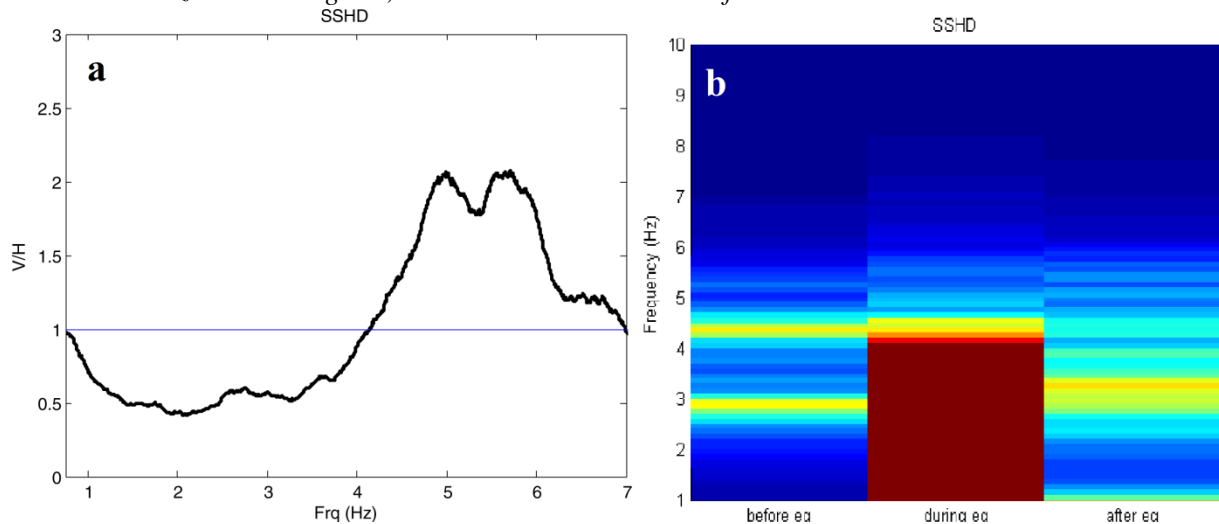


Figure 9) Analysis frequency of SSHD station located in the unknown area. (a) there is a considerable peak in 4.2–7 Hz in the V/H ratio diagram (b) there is a significant peak around 3 Hz before and after the earthquake in PSD diagram, but in after section, it is more

4.2–Polarization

Since during data acquisition a lot of artificial and cultural noise was recorded and removing all of them is impossible, our flat data may still contain artificial noise. We thus use a polarization technique to determine of the directivity of particle motion. Having a random directivity in every station means a background noise; otherwise, a specific direction is equivalent to cultural noise of a special source. Therefore, the first step in processing flow is band pass filtering of 1–6 Hz of already cleaned 3–C data in the time domain. Any time interval of 3–C data (u_x , u_y , u_z) contains N time samples. Covariances between the three components are given by:

$$C_{ij} = \left[\frac{1}{N} \sum_{s=1}^N u_i(s) u_j(s) \right] \quad \text{Eq. 1}$$

with C the covariances and:

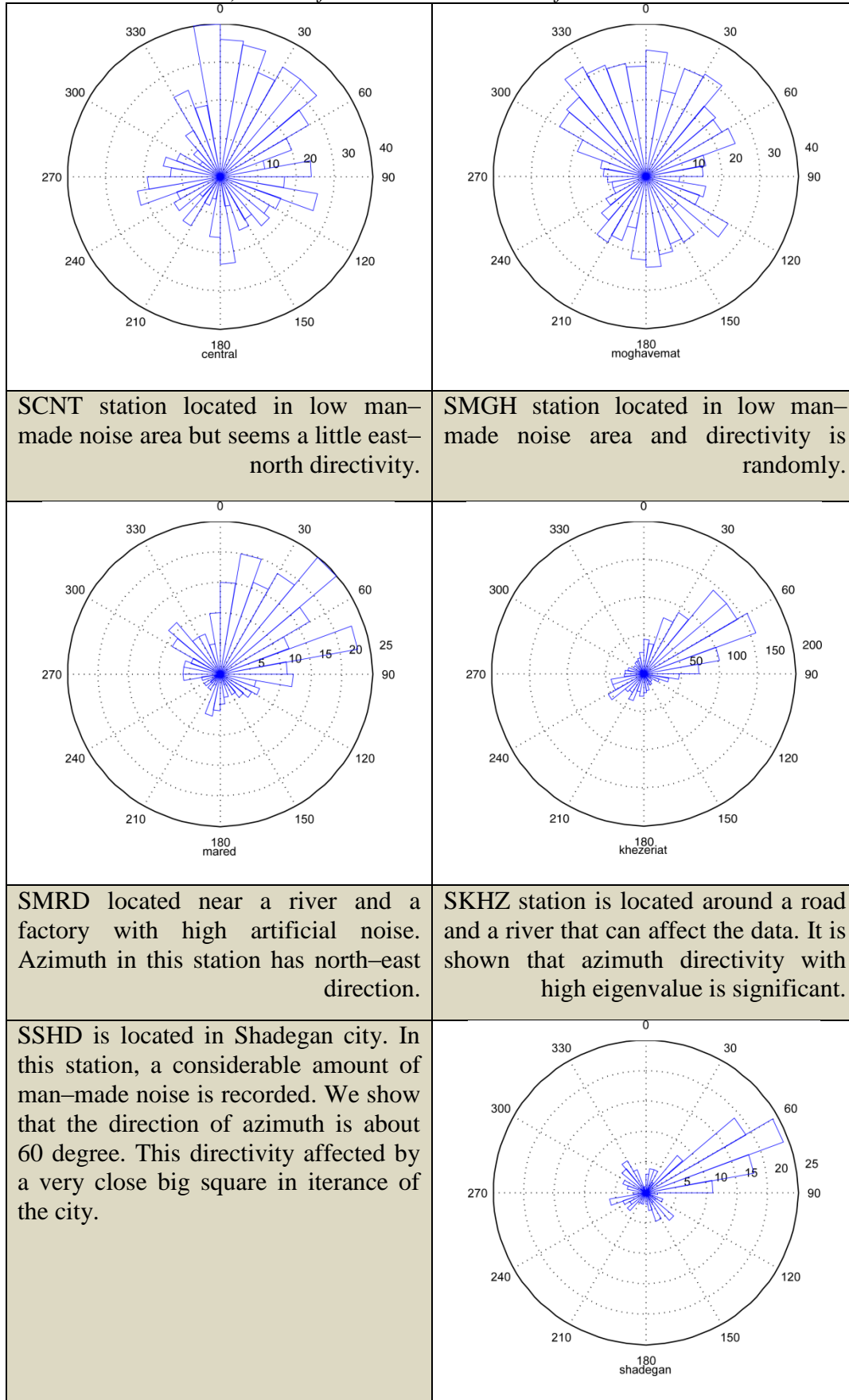
$$(C - \lambda I)P = 0 \quad \text{Eq. 2}$$

with λ the eigenvalue, $P = [p_1(x), p_1(y), p_1(z)]$ the eigenvector and I the unity matrix for 3–C data. The azimuth is specified by:

$$\theta = \tan^{-1} \left(\frac{p_1(y)}{p_1(x)} \right) \quad \text{Eq. 3}$$

where θ is the azimuth. Table 1 shows rose diagrams of the distribution of calculated azimuth for all the stations and compares them with the location of stations.

Table 1) Result of the azimuth calculation for all stations.



Since stations SKHZ, SMRD, and SSHD are too much affected by man-made noise for passive seismic data acquisition, they

pose a processing challenge. In contrast, stations SMGH and SCNT, that are less

noise affected, have useful data for the analysis.

5– Discussion

As we expect a peak between 1–6 Hz in SMGH station has been detected. Figure 5 illustrates that this station shows an acceptable peak in V/H diagram, and a distinct peak after the earthquake in PSD–IZ spectral diagram is observed. These two attributes can be properly confirmed over a known hydrocarbon reservoir in SMGH station. Accordingly, the calculation results of V/H ratio and PSD–IZ in SCNT station (Figure 1) do not claim the existence of hydrocarbon in this area. The obtained results for SMGH and SCNT stations correspond appropriately to the geological data of Darquain oil field.

There is no information available about the hydrocarbon potential for the other three analyzed stations (SKHZ, SMRD, and SSHD). Polarization analysis and station locations are shown in Table 1.

Although these three stations are very noisy and data processing isolation is very confusing but it is obviously these stations affect by a road, a factory and square internal city respectively in SKHZ, SMRD and SSHD.

The results of the data analysis of SKHZ station are illustrated in two methods in Figure 2. There are a few small peaks between 2 to 3.2 Hz in the V/H ratio spectrum, and there is a continuous peak before and after the earthquake occurrence around 3 Hz in the PSD spectrum, with the former one having a higher value. The comparison with azimuth directivity shows that the reason for these two peaks is related to the existence of cultural noise and not background noise. Therefore because of inappropriate two attributes, claim

existence of hydrocarbon beneath this station is not promising.

The result of data analysis for another station, namely SMRD, is shown in Figure 3. In V/H ratio diagram, there is only one peak in 4.2 Hz. This station is located close to a river, showing azimuth directivity (Table 1). It should be considered that there is no distinct attribute in PSD diagram; therefore hydrocarbon potential beneath this station seems unlikely.

The final studied station was SSHD which is located in Shadegan city. Based on frequency analysis conducted for this station (Figure 9), there is a distinct peak between 4 to 6 Hz and a contrasted spectrum in PSD diagram around 3 Hz considering this point that the peak is more contrasted after the earthquake rather than before it. According to Table 1, there is azimuth directivity in rose diagram that shows the data are quite distributed by noise because of urban area. Based on the two mentioned attributes, claiming the existence of hydrocarbon is not out of mind. Finally we have to mention the peaks between 1–6 Hz can also be a result of unconsolidated layer resonances which we don't have any information about such layers in this region which is a part of Arabian plate and near big Iranian river the Karon.

5– Conclusions

According to Dangel *et al* (2003) and the comparison between observations of these results with Saenger *et al* (2009) and Nguyen *et al* (2008), V/H ratio and PSD–IZ could be two attributes for locating the reservoir. In the current study, anomalies in V/H ratio and PSD–IZ attributes were observed at a location above the good known producing Darquain oil field in Iran. Results from a station located in the eastern bound of the hydrocarbon field

that is probably non-prospective show no such anomalies.

Other three stations that locate out the boundary of known Darquain reservoir there are not any considerable anomaly as we expected for hydrocarbon attributes, therefore we could not claim to existence of hydrocarbon beneath these stations with these two attributes. We recommend design a network with more stations to investigate those regions.

Acknowledgements

The authors would like to thank Dr. S. Castellaro and Dr. N. Riahi for their kind and careful comments that made the manuscript improved. Mr. Saber Shrivani and Mr. Hamid Seyedin are highly appreciated for their useful help and comments. The authors would like to thank the reviewers for their comments that help improve the paper.

References:

- AbdollahieFard I., Braathen A., Mokhtari M., Alavi S.A. 2006. Interaction of the Zagros Fold-Thrust Belt and the Arabian-type, deep-seated folds in the Abadan Plain and the Dezful Embayment, SW Iran. *Petroleum Geoscience*: 12, 347–362.
- Berberian M. 1995. Master “Blind” Thrust faults hidden under the Zagros folds: Active basement tectonics and surface morphotectonics. *Tectonophysics*: 241, 193–224.
- Dangel S., Shaepman M.E. Stoll E.P., Carniel R., Barzandji O., Rode, E.D., Singer J. M. 2003. Phenomenology of tremor like signals observed over hydrocarbon reservoirs. *Journal of Volcanology and Geothermal Research*: 128, 135–158.
- Graf. R., Schmalholz. S.M., Podladchikov. Y., Saenger. E. H. 2007. Passive low frequency spectral analysis: Exploring a new field in geophysics. *World Oil*: 228, 47–52.
- Green, A. G., Greenhalgh. S. 2009. Comment on ‘Low-frequency microtremor anomalies at an oil and gas field in Voitsdorf, Austria’ by Marc-André Lambert, Stefan Schmalholz, Erik H. Saenger and Brian Steiner. *Geophysical Prospecting*: 58, 335–339.
- Holzner. R., Eschle P., H. Zürcher, M. Lambert, R. Graf, S. Dangel, Meier, P. F. 2005. Applying microtremor analysis to identify hydrocarbon reservoirs. *First Break*: 23, 41–46.
- Konno, K., Ohmachi, T. 1998. Ground-motion characteristics estimated from spectral ratio between horizontal and vertical components of microtremor. *Bulletin of the Seismological Society of America*: 88, 228–241.
- Lambert, M., Schmalholz S. M., Podladchikov Y.Y., Saenger E.H. 2007. Low frequency anomalies in spectral ratios of single station microtremor measurements: Observations across an oil and gas field in Austria. 77th Annual International Meeting, SEG, Expanded Abstracts: 1352–1356.
- Lambert, M., Steiner B., Schmalholz S.M. Holzner R., Saenger E. H. 2006. Soft soil amplification of ambient seismic noise — Field measurements and numerical modeling of H/V ratios, EAGE Workshop on Passive Seismic, Extended Abstracts, A10.
- Lambert, M. A., Schmalholz S. M., Saenger E .K., Steiner.,B. 2009. Low-frequency microtremor anomalies at an oil and gas field in Voitsdorf, Austria. *Geophysical Prospecting*: 57, 393–411.

- Lambert, M., Nguyen A. T., Saenger E. H., Schmalholz S. M. 2011. Spectral analysis of ambient ground-motion-Noise reduction techniques and a methodology for mapping horizontal inhomogeneity. *Journal of Applied Geophysics*: 74, 100–113.
- Lambert, M. A., Schmalholz S. M., Saenger E. K., Steiner, B. 2009. Reply to comment on 'Low-frequency microtremor anomalies at an oil and gas field in Voitsdorf, Austria' by Marc-André Lambert, Stefan M. Schmalholz, Erik H. Saenger and Brian Steiner, *Geophysical Prospecting*: 57, 393–411. *Geophysical Prospecting*: 58, 341–346.
- Maleki M., Javaherian, A., Abdollahi Fard, I. 2006. High porosity anomaly with good reservoir properties in the lower Fahliyan formation (Neocomian) of Darquain Field (SW Iran) by 3D seismic: *Journal of the Earth and Space physics*: 32, 33–39
- Motiei, H. 1995. Petroleum geology of Zagros, *Treatise on the geology of Iran*. Geological Survey of Iran, Tehran.
- Nakamura. Y. 1989. A method for dynamic characteristics estimation of subsurface using microtremor on the ground surface. *Quarterly Report Railway Technical Research Institute*: 30, 25–30.
- Pujol, J. 2003. Elastic wave propagation and generation in seismology: Cambridge University Press.
- Riahi, N., Goertz, A., Birkelo, B., Saenger E. K. 2013. A statistical strategy for ambient seismic wavefield analysis: investigating correlations to a hydrocarbon reservoir. *Geophysical Journal International*: 192, 148–162.
- Rode, E. D., Nasr, H., Makhous, M., 2010. Is the future of seismic passive? *First Break*: 28, 77–81.
- Saenger, E. H., Schmalholz, S. M., Lambert, M., Nguyn, T. T., Torres, A., Metzger, S., Habiger, R. M., Müller, T., Rentsch, S., Hernández, E. M. 2009. A passive seismic survey over a gas field: Analysis of low frequency anomalies. *Geophysics*: 74, 029–040.
- Nguyen T. T., Saenger. E. H., Schmalholz S. M., Artman B. 2008. Earthquake triggered modifications of microtremor signals above and nearby a hydrocarbon reservoir in Voitsdorf, Austria. 70th EAGE Conference and Exhibition.
- Zhang H., Sarkar S., Nafi Toksöz M., Sadi Kuleli., H., Al-Kindy, F. 2009. Passive seismic tomography using induced seismicity at a petroleum field in Oman. *Geophysics*: 74, WCB57–WCB69.